Original Research Article

Design and Simulation of a Shell and Tube Heat Exchanger for a Pyrolysis Reactor

ABSTRACT

Global concern for climate change and greenhouse gases effect necessitates the promotion and development of an alternative source of energy which will drastically reduce global warming and ultimately pose lesser threat to climate change. Since the volatiles are composed of the condensable and non-condensable components, a heat exchanger is required to obtain bio-fuel from these volatiles. In this research heat exchanger was developed for optimum condensation of volatile vapour (pyro-gas) exiting in a reactor during pyrolysis process. Copper and stainless steel were selected for the development of heat exchanger tube and shell respectively. Mathematical equations were used in sizing and rating the shell and tube heat exchanger, thereby estimating the desired length, shell diameter and number of baffles. Computational Fluid Dynamic (CFD) simulation of the designed heat exchanger was done on the ANSYS software and the validation of the model was achieved by comparing the theoretical temperature with the temperature predicted from the simulation. Results from the theoretical and CFD simulation shows satisfactory similarity in terms of percentage deviation estimated as 4.68% for shell and 4.62% for tube respectively. Simulated percentage product yield for liquid (48.88% and 46.00%), and gas (9.36% and 29.12%) at 400^{o}C and 600^{o}C were slightly higher than the experimental values of liquid (47.00% and 44.00%), and gas (9.00% and 28.00%) at the same temperatures. In conclusion, the designed heat exchanger can be developed and used for the existing reactor for efficient and effective condensation for improved bio-oil yield.

Keywords: Heat exchanger, reactor, pyrolysis, bio-oil, ANSYS, simulation,

1 INTRODUCTION

Energy propels human life and also essential for continuing human development. A growing global population necessitates more energy. The world depends heavily on fossil fuels to supply its energy needs.However, as global consumption increases, these fuels, particularly oil and natural gas, will be depleted, most likely by the end of the century [1]. Furthermore, the use of fossil fuels and nuclear energy is intimately linked to environmental deterioration that endangers human health via climate change and greenhouse gas emissions [2].

Many researchers and organizations has been working to promote renewable energy sources in response to the major social, political, and economic problems that included the need for energy security and the diversification of its supplies as well as a reduction in the total dependence on fossil fuels, the incessant changes in oil prices, and growing concerns over climatic changes and environmental degradation[3]. However, this new energy paradigm also necessitates new techniques for assessing the feasibility of alternative energy sources. The introduction of alternative energy sources has resulted in a more sustainability-driven approach, necessitating advanced measurements of a wider range of criteria [4]. Whereas in the past, the success of energy carriers was primarily motivated by financial considerations, leading to preferred choice of fossil fuels such as oil.

Biomass pyrolysis has a lengthy history and significant future possibilities as interest in renewable energy grows [5]. Perhaps the first large-scale application of a gasification-related process was the pyrolysis of biomass to make charcoal. When wood became scarce due to abuse at the beginning of the eighteenth century, coke was manufactured from coal via pyrolysis [1]. According to Putra *et al.,* [6], biomass resources are abundant around the world. The majority of biomass is typically derived from palm oil, palm, corn husks, rice, and sugarcane bagasse, with significantly smaller

quantitiescoming from other sources. Depending on the source of the biomass, a variety of methods can be used to turn it into heat and electricity. These conversion processes include combustion, pyrolysis, gasification, liquefaction, anaerobic digestion, and fermentation. Because of the benefits pyrolysis has in storage, transportation, and application diversity, such as in internal combustion engines, boilers and turbines, it has garnered the most interest among these energy conversion techniques for producing liquid fuel products [5], [6].

Pyrolysis has been defined as 'the incomplete thermal decomposition of biomass, generally in the production char, condensable liquids (tar oils and acids) and non-condensable gaseous products [5]. Biomass pyrolysis is a thermal conversion process achieved by robust chemical and physical interactions between biomass and its adjacent high-temperature conditions. It is the thermal degradation either in the complete absence of oxidizing agent, or with such a limited supply that gasification does not occur to an appreciable extent or may be described as partial gasification [7].

By using pyrolysis technology, biofuel with high fuel-to-feed ratios can be produced. As a result, in recent decades, pyrolysis has drawn increased attention as a process for effectively turning biomass into biofuel [8] - [11]. Pyrolysis is the term used to describe the thermal processing of biomass without air or oxygen, to yield solid (char), liquid (bio-oil), and gaseous (bio-gas) products [12]. In this process, without air or oxygen, the thermal breakdown of organic components in biomass begins around 350°C to 550°C and can reach 700°C to 800°C [13]. Under pyrolysis conditions, the compounds of carbon, hydrogen, and oxygen in biomass decompose into smaller molecules that take the form of gases, condensable vapour (tars and oils), and solid charcoal. The molecules of the object are stretched and rattled to the point where they are broken down into smaller molecules during the pyrolysis process and this is done by heating the material to extremely high temperatures that cause intense molecular vibrations [14]. Pyrolysis is a method that can be used to reduce a large amount of highly polluting industrial waste while also creating energy and/or useful chemical compounds [15].
Many researchers including[12], [16] – [27]have worked on pyrolysis of biomass for biofuel production with little or no attention paid to the design detailsof the condensing unit or heat exchanger, where the liquid bio-oil is obtained as a result of condensation of the vapour generated from the pyrolysedbiomass. Pyrolysis condensation is a process involving the thermal decomposition of organic materials, typically in the absence of oxygen, resulting to the formation of volatile compounds. These compounds are then condensed to obtain valuable products such as bio-oil, gases, and char [28; 29]

There are varieties of heat exchangers available for this purpose, ranging from straightforward indirect contact heat exchangers to more intricate quenching columns. Examples are Shell and Tube Heat Exchangers, Plate Heat Exchangers, Finned Tube Heat Exchangers, Double Pipe Heat Exchangers, Air Cooled Heat Exchangers, and Adiabatic Wheel Heat Exchangers [26]. This research is therefore focusedto design and simulate a simple shell and tube water cooled energy release device(heat exchanger) for efficient and effective condensation, and improved bio-oil yield in a pyrolysis reactor.

2. RESEARCH METHODOLOGY

2.1 Materials

This research considered the design of a cooling unit(exchanger) fora pyrolysis reactor developed by [5]. The exchanger designed is the shell and tube (straight single-pass) type, with water as the cooling medium. The exchanger is also referred to as shell and tube heat exchanger, because small diameter tubes are arranged in large diameter tube known as the shell. Copper, a material with high thermal conductivity was chosen for the tubes in order to maximize heat transfer efficiency and prevent deterioration from corrosion over a long period of time under operational circumstances such as pressures and temperatures. The material properties for the tube (copper), shell (stainless steel), and fluids (pyro-gas and water) are defined as shown in Table 1. Copper was selected for the tube due its high thermal conductivity, necessary for improved heat transfer between the hot pyro-gas and cold water. Stainless steel with low thermal conductivity on the other hand was selected for the shell side due to its ductility, toughness and malleability and more so, heat loss to the surrounding is to be prevented and hence the wall of the steel is assumed to be adiabatic.

Table 1: Thermo-physical properties of selected tube materials and fluids[29], [30]

Name	Density, ρ (kg/m^3)	Specific heat, c_p (J/kgK)	Thermal Conductivity, k $(W/m.K)$	Dynamics viscosity, μ $(N.s/m^2)$
Copper,	8960	385	401	-
Stainless Steel	8055	480	15.1	-
Water	997.13	4182	0.61	0.891×10^{-3}
Pyro-gas	106.7	2015.8	0.182	2.1856×10^{-5}

2.2 Design Procedure

The procedure adopted to design the shell and tube heat exchanger include: selection of fluids to be placed on the tube and shell sides respectively, selection of tube and shell materials based on physical properties of the two streams of fluid, selection of geometric parameters for the heat exchanger, specifying the flow rates and temperatures of the streams both at inlets and outlets, determination of the exchanger heat duty based on the parameter declared, estimation of the quantity of baffles to be used and its spacing, determination of both the tube and shell heat transfer coefficients and determination of the pressure drop on the tube and shell side of the exchanger. Some selected parametric values for the design are as shown in Table2.

Table 2: Selected parameters for design of the heat exchanger

Description	Value
Capacity of reactor	17.4 litre
Heating element	2.5 Kw
Temperature of pyro-gas at tube inlet, $\boldsymbol{t_{\mathrm{hit}}}$	500℃ $(773\ K)$
Temperature of water at shell inlet, $\boldsymbol{t_{cis}}$	25℃ $(298\ K)$
Expected temperature of water at shell outlet, $\boldsymbol{t_{cos}}$	95℃ $(373\ K)$
Overall heat transfer coefficient, $\boldsymbol{U}$	665
Mass flow rate of pyro-gas at tube inlet, $\dot{\mathbf{m}}_{\mathbf{t}}$	$0.1\ kg/s$
Mass flow rate of water at shell inlet, $\dot{\mathbf{m}}_{\mathbf{s}}$	$0.3\ kg/s$
inner diameter of tube, $\boldsymbol{D_{\mathrm{i}}}$	$0.012\ m$
Outer diameter of tube, $\boldsymbol{D_{\mathrm{o}}}$	$0.016\ m$
Number of tube, $\boldsymbol{N_{\mathrm{t}}}$	7
Baffle thickness, $\boldsymbol{t_b}$	$0.003\ m$

2.3 Design Consideration

The water-cooled condenser designed in this research is for an existing pyrolysis reactor developed by [5]. The reactor has a capacity of 17.4 litres, with Akure clay as its refractory material.It is encased in a steel frame with outlet vapour temperature of 500℃ and minimum flow rate of 0.1kg/s. Heat is generated electrically by two heating elements rated at 2.5 kW each. It was equipped with a temperature controller and thermocouples for varying and measuring the temperaturesin the chamber and the reactor.The heat exchanger was designed assuming minimum vapour mass flow rate of 0.1kg/s and hot vapour with temperature of 500 ℃ which will drop the temperature when cooled, from the reactor flowing into the tube, and releasing heat to the cold water with assumed temperature of 25 ℃ passing through the shell. Minimum water mass flow rate of 0.3 kg/s was selected for the water and the water was expected to cool down the temperature of the vapour. At this temperature, the vapour would have cooled down satisfactorily while still in vapour state. Further cooling of the vapour is expected to be obtained by placing the condensate collector in an ice-bath to obtain the bio-fuel.

The diameter of tube was selected based on Tubular Exchanger Manufacturing Association (TEMA) standards [31], that standard tube outer diameter should be between 0.00635 and 0.0508 m. According to Thulukkanam[32], small tube diameters produces high heat transfer coefficient and are suitable for effective heat transfer. Hence in this research, the inner diameter of tube selected was 0.012 m with an outer diameter of 0.016m, and the selected number of tube and baffle thickness are 7 and 0.003m respectively. Few number of tubes was selected because a small heat exchanger will be designed which will be complemented by another heat exchanger for final cooling to get a

condensedbio-oil. The battle thickness was selected as recommended by TEMA standards. During the design, some parameters were chosen based on the design criteria, standards and operating conditions. Summary of the estimated parameters are as shown in Table 3.

Table 3: Summary of estimated parameters for the heat exchanger

Description	Value
Heat transfer rate, $\mathbf{Q}$	$87824\ W$
Temperature of pyro-gas at tube outlet, $\boldsymbol{T_{hot}}$	$125.5℃\ (K)$
Average temperature of shell-side fluid, $\boldsymbol{T_{savg}}$	$60℃\ (K)$
Average temperature of tube-side fluid, $\boldsymbol{T_{tavg}}$	$312.7℃\ (K)$
Tube wall temperature, $\boldsymbol{T_w}$	$186.4℃\ (K)$
Total surface heat transfer area of tube, $\mathbf{A}$	$0.6045\ \mathrm{m}^2$
Effective mean temperature difference, $\Delta\mathbf{T_{LM}}$	$218.48℃\ (K)$
Logarithmic mean temperature difference, $\Delta\mathbf{T_{LMTD}}$	$218.48℃\ (K)$
Length of the heat exchanger, $\boldsymbol{L}$	$1.718\ m$
Tube pitch size, $\boldsymbol{P_T}$	$0.02\ m$
Shell inner diameter, $\boldsymbol{D_s}$	$0.064\ m$
Central baffle spacing, $\boldsymbol{B}$	$0.0352\ m$
Inlet baffle spacing, $\boldsymbol{B_i}$	$0.0373\ m$
Outlet baffle spacing, $\boldsymbol{B_o}$	$0.0373\ m$
Number of baffles, N_b	44
Shell equivalent diameter, $\mathbf{D_e}$	$0.0158\ m$
Reynolds number for shell side fluid, $\mathbf{Re_s}$	11819
Reynolds number for tube side fluid, $\mathbf{Re_t}$	17343
Cross-sectional flow area of tube, $\mathbf{A_c}$	$0.000452\ \mathrm{m}^2$
Shell side fluid pressure drop, $\Delta\boldsymbol{P_s}$	$7196.6\ Pa$
Tube side fluid pressure drop, $\Delta\boldsymbol{P_t}$	$27.49\ Pa$

2.4 Design Calculation

Standard equations (1-12) were used in the design of the heat exchanger

$$\mathrm{Q} = \dot{\mathrm{m}}_\mathrm{t}\mathrm{c}_\mathrm{pt}(\mathrm{T}_\mathrm{hot} - \mathrm{T}_\mathrm{hit}) = \dot{\mathrm{m}}_\mathrm{s}\mathrm{c}_\mathrm{ps}(\mathrm{T}_\mathrm{cis} - \mathrm{T}_\mathrm{cos})\text{[33]} \quad (1)$$

$$\Delta\mathrm{T}_\mathrm{LM} = F.\Delta\mathrm{T}_\mathrm{LMTD}\ \text{[34]} \quad (2)$$

$$\Delta\mathrm{T}_\mathrm{LM} = 1 * \Delta T_{LMTD}\ \text{[32]} \quad (3)$$

$$\Delta\mathrm{T}_\mathrm{LMTD} = \frac{(\mathrm{T}_\mathrm{hot} - \mathrm{T}_\mathrm{cos}) - (\mathrm{T}_\mathrm{hit} - \mathrm{T}_\mathrm{cis})}{ln(\mathrm{T}_\mathrm{hot} - \mathrm{T}_\mathrm{cos})/(\mathrm{T}_\mathrm{hit} - \mathrm{T}_\mathrm{cis}))}\ \text{[34]} \quad (4)$$

$$\mathrm{A} = \pi D_0 N_t L \quad \text{[32]} \quad (5)$$

$$L = \frac{\mathrm{A}}{\pi D_0 N_t} \quad (6)$$

$$P_T = PR \times D_o\ \text{[33]} \quad (7)$$

$$D_s = 0.637\sqrt{\frac{CL}{CTP}}\left[\frac{A(PR)^2 D_o}{L}\right]^{1/2} \quad (8)$$

$$N_b = \frac{L}{B + t_b} - 1 \quad (9)$$

$$B = Percentage \times D_s \quad (10)$$

$$B_i = B_o = \frac{L - ((N_b - 1)(B + t_b))}{2} \quad (11)$$

$$B_c = percentage\ cut \times D_s \quad (12)$$

where: Q is the heat transfer rate (W); $\dot{\mathrm{m}}_\mathrm{s}$ and $\dot{\mathrm{m}}_\mathrm{t}$ are shell and tube sides mass flow rate (kg/s); $c_{pt}\ and\ c_{ps}$ are tube and shell sides fluid specific heat capacity (J/kgK); T_{cos}, T_{cis}, , T_{hot} and T_{hit} are shell outlet, shell inlet, tube outlet and tube inlet temperatures ($^\mathrm{o}$C); $\Delta\mathrm{T}_\mathrm{LMTD}$ is Logarithmic Mean Temperature Difference (LMTD) ($^\mathrm{o}$C); $\Delta\mathrm{T}_\mathrm{LM}$ is Effective Mean Temperature Difference ($^\mathrm{o}$C); F is correction factor for LMTD; N_t is Number of tubes; D_s is shell's inside diameter (m); L is the length of the heat exchanging tube (m); D_o is tube's outside diameter (m); A is thetotal surface area of tube

(m^2); CTP is Tube Count Calculation Constant; CL is tube layout constant;$t_b$is baffles thickness (m), B is the central baffle spacing; B_i and B_o are inlet and outlet baffles' spacing respectively.

2.5 Model Governing Equation

The flow of fluid inside the heat exchanger was governed by the continuity, the momentum, and the energy equations; Finite Element was used to discretize the equations. It was assumed that water is both Newtonian and incompressible, with constant thermophysical properties. The continuity, the momentum, and the energy equations are as given equations (13) to (15) [35]

$$\frac{\partial(\rho u_i)}{\partial x_i} = 0 \tag{13}$$

$$\frac{\partial(\rho u_i u_j)}{\partial x_j} = -\frac{\partial P}{\partial x_i} + \frac{\partial}{\partial x_j}\left[\mu\left(\frac{\partial u_i}{\partial x_j} + \frac{\partial u_j}{\partial x_i}\right) - \frac{2}{3}\mu\frac{\partial u_i}{\partial x_i}\delta_{ij} - \rho\overline{u_i' u_j'}\right] \tag{14}$$

$$\frac{\partial}{\partial x_j}\left(\rho u_j c_p T\right) = \frac{\partial}{\partial x_j}\left(\lambda\frac{\partial T}{\partial x_j} + \frac{\mu_t}{\sigma_{h,t}}\frac{\partial\left(c_p T\right)}{\partial x_j}\right) + u_j\frac{\partial P}{\partial x_j} +$$

$$\left[\mu\left(\frac{\partial u_i}{\partial x_j} + \frac{\partial u_j}{\partial x_i}\right) - \frac{2}{3}\mu\frac{\partial u_i}{\partial x_i}\delta_{ij} - \rho\overline{u_i' u_j'}\right]\frac{\partial u_i}{\partial x_j} \tag{15}$$

The Reynolds stresses were modelled using Boussinesq hypothesis that relates Reynold stress to the mean velocity gradient as given in equation (16)

$$-\rho\overline{u_i' u_j'} = \mu_t\left(\frac{\partial u_i}{\partial x_j} + \frac{\partial u_j}{\partial x_i}\right) - \frac{2}{3}\left(\rho k + \mu_t\frac{\partial u_k}{\partial x_k}\right)\delta_{ij} \tag{16}$$

where k is the turbulent kinetic energy per unit mass given by equation (17):

$$k = \frac{1}{2}\left(\overline{u'^2} + \overline{v'^2} + \overline{w'^2}\right) \tag{17}$$

To obtain the optimum prediction of turbulence, the accuracy of two different turbulence models (Realisable $k-\varepsilon$ model and RNG $k-\varepsilon$ model) were adopted [35].The turbulent energy and turbulent dissipation rates in the realisable$k-\varepsilon$ model are given in equations (18) and (19) respectively.

$$\frac{\partial}{\partial t}(\rho k) + \frac{\partial}{\partial x_j}\left(\rho k u_j\right) = \frac{\partial}{\partial x_j}\left[\left(\mu + \frac{\mu_t}{\sigma_k}\right)\frac{\partial k}{\partial x_j}\right] + G_k - \rho\varepsilon \tag{18}$$

$$\frac{\partial}{\partial t}(\rho\varepsilon) + \frac{\partial}{\partial x_j}\left(\rho\varepsilon u_j\right) = \frac{\partial}{\partial x_j}\left[\left(\mu + \frac{\mu_t}{\sigma_\varepsilon}\right)\frac{\partial\varepsilon}{\partial x_j}\right] + \rho C_1 S\varepsilon - \rho C_2\frac{\varepsilon^2}{k+\sqrt{v\varepsilon}} \tag{19}$$

where $G_k$is the generation of turbulent kinetic energy; c_1, C_2 are constants; and μ_t is the turbulent velocity.

2.6 Computational Fluid Dynamics (CFD) Simulation

In order to validate the designed details of the heat exchanger, its 3D model was developed and simulated using SolidWorks2014 and ANSYS FLUENT 14.0 software packages respectively [36], [37]. The complete model comprises the shell fluid (water) domain, tube fluid (pyro-gas) domain, the tube and baffle (copper) domain. Since adiabatic condition is expected on the shell wall, the shell model is not required. An imaginary wall is assumed to be on the surface of the shell fluid domain with zero heat flux assigned to it, hence indicating no heat is lost across the wall. Steady state heat transfer simulation was considered as in the theoretical design, to predict the outlet temperatures on the tube and shell sides as shown in Figures 1a and b, 2a and b and 3a and b respectively.

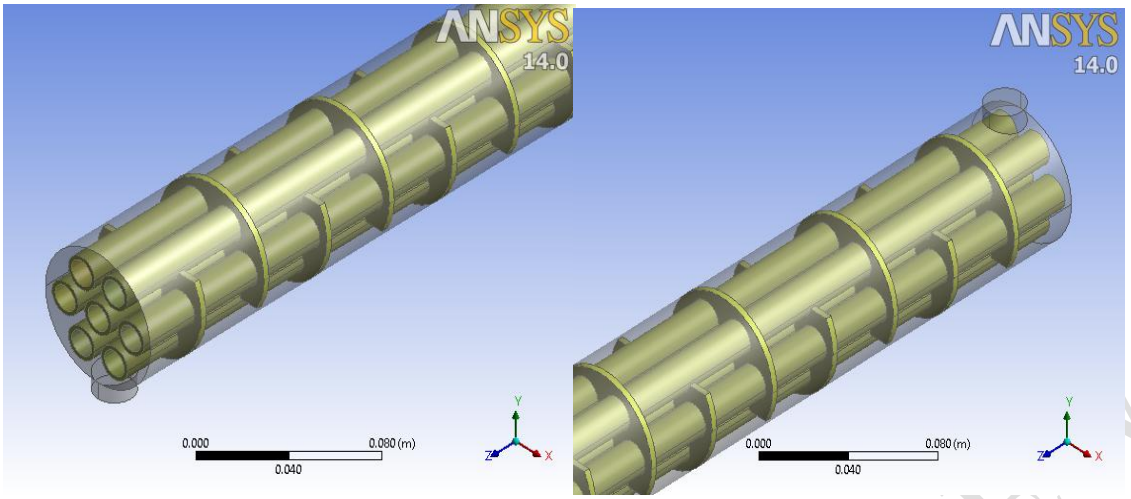

Figure 1: (a) Model with first Inlet/Outlet side **(b) Model with second Inlet/Outlet side**

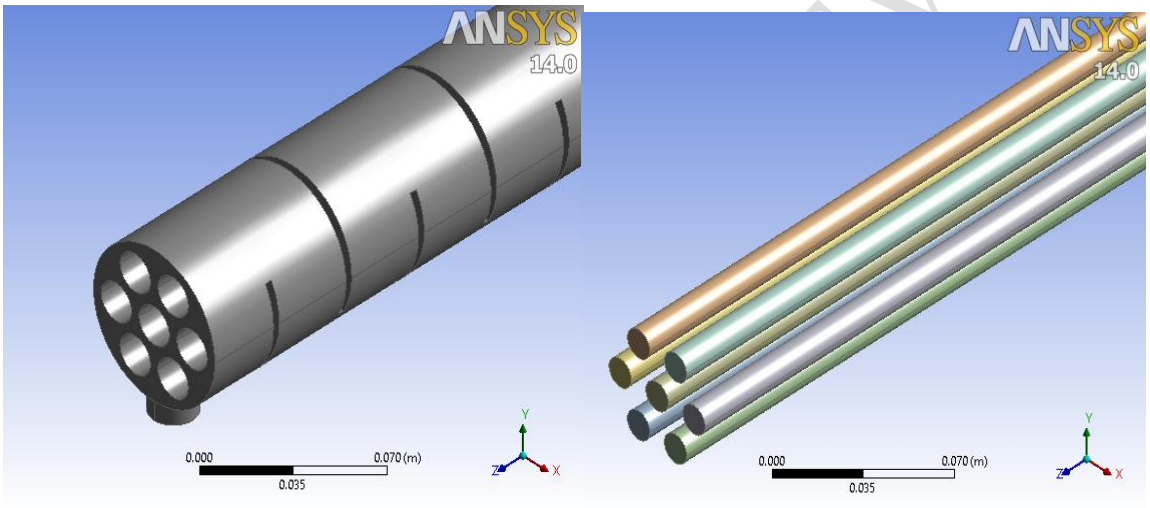

Figure 2: (a) Shell fluid (Water) domain (b) Tube fluid (Pyro-gas) domain

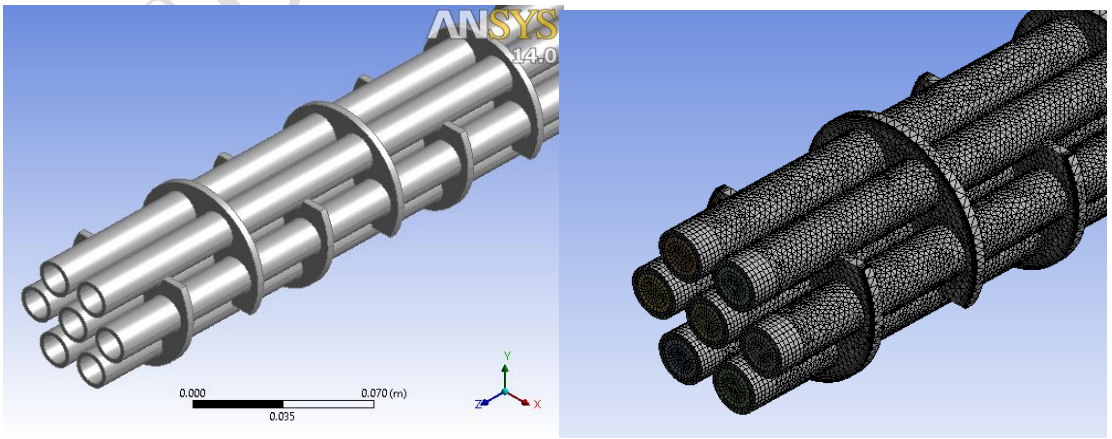

Figure 3: (a) Tube and baffles (Copper) (b) Meshed Tube and Baffles

2.6.1 Grid independence study

Four distinct meshing element counts of approximately 6.8, 7.3, 8.4, and 10.2 million were constructed and utilized to study the independence of model outputs from meshing. The results showed that 8.4 million elements have a 2% lower degree of independence than 10.2 million elements. Therefore, as shown in Figure 4, the adopted grid number (elements) in the computational domain was around 8.4 Million in order to maintain abalanced trade-off between convergence time and solution correctness.

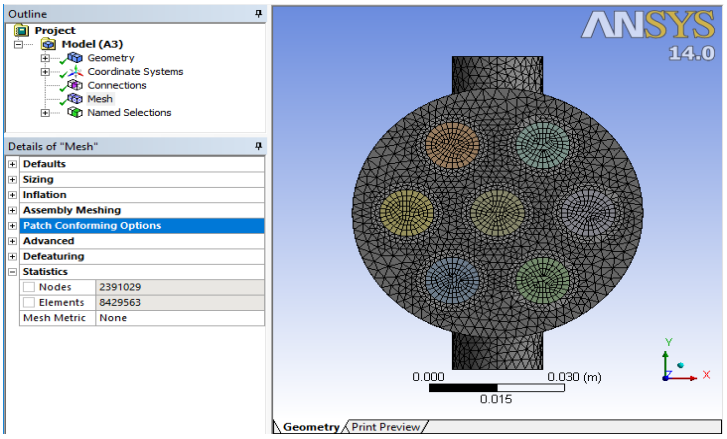

Figure 4: Front view of the meshed model with mesh details

2.6.2 Simulation solution procedure

ANSYS release 14.0, a piece of commercial CFD software, was used to implement the numerical simulation. ANSYS-FLUENT's CFD code, which employs the finite volume technique (FVM), was used to resolve the governing equations and boundary conditions [30].

Structured hexahedral elements in the walls' normal directions were used to isolate the computational domain. The SIMPLE (Semi Implicit Pressure Linked Equations) technique was used to couple pressure and velocity. The boundary conditions and governing equations were integrated over the computational domain using second-order up-wind methods. The near-wall regions were modeled using the improved wall function. The scaled residual values were specified to be less than 10^{-4} for continuity equation, fewer than 10^{-6} for velocity, turbulent kinetic energy and dissipation rate, and less than 10^{-7} for energy respectively, for the convergence condition to be satisfied.

3. RESULTS AND DISCUSSION

Mathematical equations were used to size and rate the exchanger, thereby estimating the desired length, diameter and number of baffles. Sizing the exchanger deals with estimation of geometric size and rating considers the determination of pressure drop and coefficient of heat transfer of the fluids.

3.1 CFD simulation results

The combined 3-D model (material, component, fluid flow and geometry combinations) of the designed shell and tube heat exchanger used for the simulation consists of four major parts namely, tube and baffle domain (solids), and pyro-gas and water domain (fluids). The domains were meshed using fine mesh options and the front view, showing the seven tubes, and shell inlet and outlet pipes can be seen in Figure 5. Similarly, meshed tubes and baffles are shown in Figure 6. The simulation results are shown in Figures 7 to 10 while Table 4 shows the verification of theoretical and simulation results respectively.

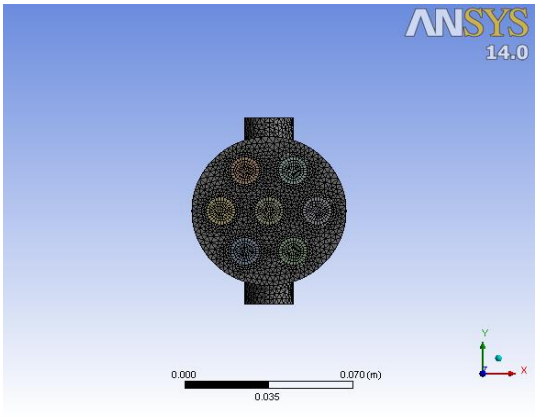

Figure 5: Meshed complete model

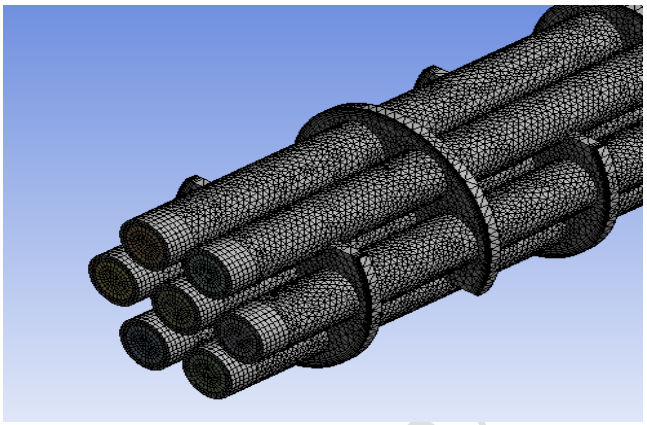

Figure 6: Meshed tube and baffle model

3.2 Verification of Theoretical and Simulation Results

For console display, area-weighted average static temperature of shell inlet and outlet, and tube inlet and outlet were computed. At the inlets, the initial selected temperatures were imputed, while at the outlet were the computed in FLUENT. Static temperature contours of the hot pyro-gas at the seven tubes inlets as shown in Figure 7, with the legend showing different level of temperature in Kelvin (K). As the hot pyro-gas loses heat to water; its temperature drops. Figure 8 shows the contour of temperature for the cooled pyro-gas at the tube outlets.

Similarly, the temperature contour on the shell inlet is shown in Figure 9. In this case, water absorbs heat from the pyro-gas, thereby increasing the shell outlet temperature as shown in Figure 10.

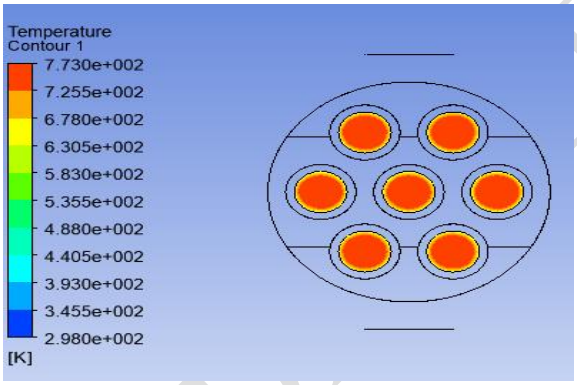

Figure 7: Static temperature contours at tube inlets

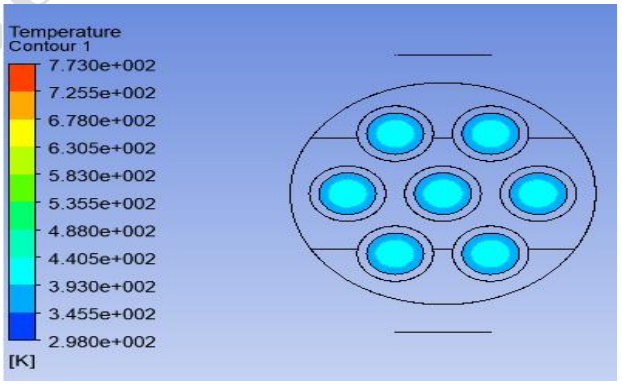

Figure 8: Static temperature contours at tube outlets

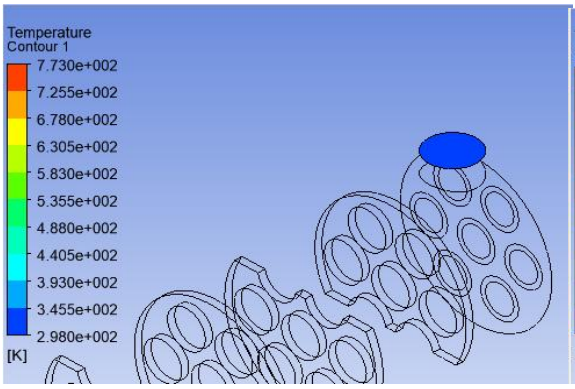

Figure 9: Static temperature contour at shell inlet

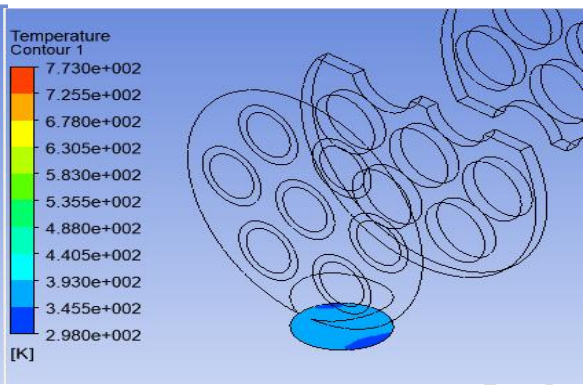

Figure 10: Static temperature contour shell outlet

3.3 Simulation Validation

The validation of the model was achieved by comparing the theoretical temperature with the temperature predicted from the simulation. The percentage deviation between the theoretical and simulated results was used to ascertain the accuracy of the simulated results obtained in comparison with the theoretical values. These results are presented in Table 4.

Table 4: Validation of the simulation tests

Parameter	Temperature (℃)		Deviation (%)
	Theoretical	Simulation	
Shell outlet	95	99.45	4.68
Tube outlet	125.5	119.7	4.62

The estimated percentage deviations for the tube side and shell side are 4.62 and 4.68% respectively. This deviation of the simulation from the experimental data might be due to human error in handling, and as well suggested that the coldness of the cooling water should be enhanced.

The validation also compared the percentage product yield (liquid and gas). Experimental data [5] was used to predict product yields from simulation at to different temperatures. Obtained results are presented in Table 5

Table 5: Percentage Yield of Products

Reactor Temperature ^{o}C	Percentage Experimental Yield (%)		Percentage Simulation Yield (%)	
	Liquid	Gas	Liquid	Gas
400	47.00	9.00	48.88	9.36
600	44.00	28.00	46.00	29.12

Product percentage yield from simulation are slightly higher than the experimental values. The results also revealed that liquid yield decreases with increase in temperature, while more of gas is produced at higher temperatures.

4. CONCLUSION

In this research, the design and simulation of a heat exchanger for the condensation of pyrolysis products were carried out. Performance evaluation was carried out usingCFD tool. Results from the theoretical and CFD simulation shows satisfactory similarity in terms of percentage deviation estimated as 4.68% for shell and 4.62% for tube respectively. Simulated percentage product yield for liquid (48.88% and 46.00%), and gas (9.36% and 29.12%) at 400^{o}C and 600^{o}C were slightly higher

than the experimental values of liquid (47.00% and 44.00%), and gas (9.00% and 28.00%) at the same temperatures.Therefore, it was inferred that the designed heat exchanger can be developed and used for the existing reactor for efficient and effective condensation for improved bio-oil yield.

REFERENCES

[1] Vamvuka, D. (2011): “Bio-oil, solid and gaseous biofuels from biomass pyrolysis processes—An overview”. *International Journal of Energy Research*35:835–862

[2] Anurita S., Yu Ling W, Kuan S. K., Wei-Hsin C., Pau L. S. (2022) "Biochar production via pyrolysis of citrus peel fruit waste as a potential usage as solid biofuel", *Chemosphere*, 294, 133671

[3] Perimenis A., Walimwipi H., Zinoviev S., Muller-Langer F., and Miertus S. (2011): “Development of a decision support tool for the assessment of biofuels”. *Energy Policy,* 39: 1782-1793, Elsevier.

[4] Mogaji, T. S., Akinsade, A. and Akintunde, M. A. (2019): Pyrolysis of Sugarcane Bagasse for Bio-Oil Production. *FUTA Journal of Engineering and Engineering Technology (*FUTAJEET) 13 (2) (150-157)

[5] Akinola, A. O. (2012): Design of a Thermochemical Reactor for Conversion of Selected Wood Biomass to Fuel aStationary Diesel Engine. Unpublished PhD Thesis in the Department of Mechanical Engineering, the Federal University of Technology, Akure, Nigeria.

[6] Putra, N., Abdullah, N.A., Hakim, I., and Koestoer, R. A. (2017): “A Review of Improvements to The Liquid Collection System Used in The Pyrolysis Process for Producing Liquid Smoke”, International Journal of Technology 7: 1197-1206.

[7] Xia C., Cai L., Zhang H., Zuo L., Shi S.Q., Lam S.S. A review on the modeling and validation of biomass pyrolysis with a focus on product yield and composition. Biofuel Research Journal 29 (2021) 1296-1315. DOI: 10.18331/BRJ2021.8.1.2

[8] Rasul, M.G., Jahirul, M.I., Chowdhury, A.A, and Ashwatch, N. (2012): Biofuel Production through Biomass Pyrolysis, *Energies5*, 4952-5001.

[9] Ryu, H. W., Kim, D. H., Jae, J., Lam, S. S., Park, E. D. and Park, Y. K. (2020): Recent advances in catalytic co-pyrolysis of biomass and plastic waste for the production of petroleum-like hydrocarbons. *Bioresources Technology*. 310:123473. doi: 10.1016/j.biortech.2020.123473.

[10] Hassan H, Lim, J. and Hameed, B. H (2016): Recent progress on biomass co-pyrolysis conversion into high-quality bio-oil. (2016): *Bioresources Technology*. 221:645-655. doi: 10.1016/j.biortech.2016.09.026.

[11] Suriapparao, D. V, Vinu, R., Shukla, A. and Haldar, S. (2020): Effective deoxygenation for the production of liquid biofuels via microwave assisted co-pyrolysis of agro residues and waste plastics combined with catalytic upgradation. *Bioresources Technology*. 302:122775. doi: 10.1016/j.biortech.2020.122775..

[12] Akinola A. O., Eiche J. F.,Owolabi P. O. and Elegbeleye A. P. (2018): Pyrolytic Analysis of Cocoa Pod for Biofuel Production. *Nigerian Journal of Technology* (NIJOTECH) 37, pp. 1026 – 1031

[13] Fisher, T., Hajaligol, M., Waymack, B. and Kellogg, D. (2002): “Pyrolysis behaviour and kinetics of biomass derived materials”. *Journal of Applied Pyrolysis,*62, 331–349.

[14] Pyrocrat, (2007):Industrial Pyrolysis of Waste Plastic and Tyres Retrieved From www.pyrolysisplant.com

[15] Natalia J., Tomas B., and Maria C. (2013):The Effect of Temperature Pyrolysis Process of Used Tyres on the Quality of Output Products. *acta mechanica et automatica, 7*(1):.20-24.

[16] Igbinadolor, R. (2012). "Fermentation of Cocoa Pod Husk (Theobrama Cacao) and its Hydrolysate for Ethanol production using improved starter culture" Unpublished PhD Thesis at the University of Ibadan, Ibadan, Nigeria.

[17] Adeyi, O. (2010): Proximate Composition of some Agricultural Wastes in Nigeria and their Potential use in Activated Carbon Production. Journal of Environmental Science and Management 14: 55-58.

[14] Mason, L., Gustafson, R., Calhaun, J., Lippke B. and Raffaeli, N. (2009): Wood to Energy in Washington. The College of Forest Resources, University of Washington. Report to the Washington State Legislature.

[18] Cruz G., Pirila M., Huuhtanen M., Carrion L., Alvarenga E. and Keiski R. L. (2012): Production of Activated Carbon from Cocoa Pod Husk. *Journal of Civil and Environmental Engineering* 2:109

[19] Odesola I. F. and Owoseni T. A. (2016): Development of Local Technology for a Small-Scale Biochar Production Processes from Agricultural Wastes. *Journal of Emerging Trends in Engineering and Applied Sciences* (JETEAS) 1 (2): 205-208.

[20] Ward-Doria M., Arzuaga-Garrido J., Ojeda K. A., and Sanchez, E. (2016): Production of Biogas from Acid and Alkaline Pretreated Cocoa Pod Husk. *International Journal of ChemTech Research* 9(11), 252-260.

[21] Gooty, A. T., Li, D., Berruti, F. and Briens, C. (2014): "Kraft-Lignin pyrolysis and fractional condensation of its bio-oil vapours".*Journal of Analytical and Applied Pyrolysis.* 106: 33-40

[22] Vukic, M., Tomic, M., Zivkovic, P.. and Ilic, G. (2014): Effect of Segmental Baffles on the Shell and Tube Heat Exchanger Effectiveness. *Scientific Paper,Hemijska Industrija 68.* 171 – 177.

[23] Dubey, V. V. P., Verma, R. R., Verma P. S. and Srivastava, A. K. (2014): Performance Analysis of Shell and Tube Heat Exchanger under the Effect of Varied Operating Condition. *IOSR Journal of Mechanical and Civil Engineering 2*(3) Ser. IV, pp 08 – 17.

[24] Musilim, A.A., Nwagwo, A. and Uche, O. K. (2017): Effect of baffle cut sizes on temperature and pressure drop at various mass flow rate in a shell and tube heat exchanger. *International Journal of Engineering, Science and Mathematics* 6(1): 1 – 10.

[25] Kansal S. and Shabahat, F. (2014): "Design and performance evaluation of shell and tube heat exchanger using CFD simulation", *International Journal of Research And Technology*, 3(7): 1663-1666.

[26] Zena K. K., Kassimmuna S., Adel, H. and Abdul, Y. (2016): "CFD study for cross flow heat exchanger with integral finned tube", *International Journal of Scientific and Research Publication*, 6(6) 668-677.

[27] Bridgwater, A. V. (2012): Review of fast pyrolysis of biomass and product upgrading. *Biomass and Bioenergy*, 38, 68-94.

[28] Chiaramonti, D., Prussi, M., Buffi, M., Rizzo, A. M. and Pari, L. (2013): Review and experimental study on pyrolysis and hydrothermal liquefaction of industrial plastic waste. *Energy & Fuels*, 27(6), 3424-3436.

[29] Massoud, M. (2005): Engineering Thermofluids: Thermodynamics, Fluid Mechanics and Heat Transfer. 20742, College Park, MD, USA.

[30] Nwokolo, N. L. (2016): Design, Manufacture and Performance Evaluation of Waste Heat recovery unit in a Gasification Plant. Unpublished PhD Thesis at the Faculty of Science and Agriculture, the University of Forte Hare.

[31] TEMA (1999): Standards of the Tubular Exchanger Manufacturers Association. 8th Edition, Tubular Exchanger Manufacturers Association Inc.

[32] Thulukkanam, K. (2013): Heat Exchanger Design Handbook, 2nd Edition. Taylor & Francis Group, New York.

[33] Kakac, S.. Liu, H. and Pramuanjaroenkij, A. (2012): Heat Exchanger: Selection, Rating and Thermal Design, Third Edition, CRC Press, Taylor and Francis Group

[34] Cengel, Y.A. (2005): "*Heat Transfer: A Practical Approach",* 2nd ed., McGraw-Hill, 2003. ISBN 0072458933

[35] Oni, T.O. and Paul, M.C. (2016): CFD investigation of the impacts of variation in geometry of twisted tape on heat transfer and flow characteristics of water in tubes. *Heat Transfer: Asian Research*. 45(5), 482-498.

[36] ANSYS (2006): ANSYS FLUENT Help Manual, Release 16.1. 2006.

[37] Ba, T. N., Ngoc, B. P., Embong, A. M., Nhu, N. N. T. Xuan, A. N. S., Trung, N. H., Abdul-Kadir, N. A., Nguyen, T., and Pham, L. H. P (2021): Simulation of shell and tube heat exchanger using COMSOL software. ICCFB 2021 IOP Conference Series: Earth and Environmental Science 947 (2021) 012008 *IOP Publishing* doi:10.1088/1755-1315/947/1/012008